# Short-term photoacclimation effects on photoinhibition of phytoplankton in the Drake Passage (Southern Ocean)

Anne-Carlijn Alderkamp [a,b,*], Véronique Garcon [c], Hein J.W. de Baar [b,d], Kevin R. Arrigo [a]

[a] Department of Environmental Earth System Science, Stanford University, Stanford, CA 94305, USA
[b] Department of Ocean Ecosystems, Energy and Sustainability Research Institute Groningen, University of Groningen, 9747 AG Groningen, The Netherlands
[c] Laboratoire d'Etudes en Géophysique et Océanographie Spatiales, Toulouse, FR-31055, France
[d] Royal Netherlands Institute for Sea Research, 1790 AB Den Burg, Texel, The Netherlands

## ARTICLE INFO

## ABSTRACT

We assessed whether short-term photoacclimation responses of natural phytoplankton populations in the Drake Passage (Southern Ocean) were affecting protection from photodamage as cells are mixed up to the surface from depth. To this end, we measured phytoplankton fluorescence characteristics and their ratio of xanthophyll cycle pigment to photosynthetic pigments within the upper mixed layer (UML) and in short-term deck incubation experiments. Phytoplankton within the UML photoacclimated by increasing their ratio of xanthophyll cycle (diadinoxanthin [dd] and diatoxanthin [dt]) pigments to chlorophyll $a$. The photoacclimation processes observed within the UML did, however, not influence the protection of phytoplankton from photodamage during short-term near-surface irradiance experiments. Exposure to near-surface irradiance resulted in photodamage in all experiments, regardless of the phytoplankton community composition and irradiance levels. Incubating phytoplankton for six hours at either 2% or 50% of surface irradiance prior to exposure to near-surface irradiance did not alter the photodamage characteristics. This suggests that short-term photoacclimation processes within the UML are not adequate to protect phytoplankton from photodamage when cells are mixed up to the surface from depth, and that repair of damaged photosystems is crucial for maintaining photosynthesis under fluctuating irradiance conditions, even at very low mean irradiance levels. Likely, continuously operating photoacclimation processes offset to some extent the negative effects of photodamage on photosynthetic performance, albeit with increased metabolic costs.

© 2011 Elsevier Ltd. All rights reserved.

## 1. Introduction

The Antarctic Circumpolar Current (ACC) is part of the largest of the high nutrient-low chlorophyll (HNLC) regions; oceanic regions with high concentrations of inorganic macronutrients and a low phytoplankton biomass (Chisholm and Morel, 1991). Primary productivity in the ACC is largely controlled by the availability of iron (Fe), the main sources of which are dust deposition and upwelling of the prevailing eastward transport of the ACC (Pollard et al., 2002; Strass et al., 2002; Hiscock et al., 2003). In addition, phytoplankton productivity may be light limited in many areas of the ACC, since weak water column stratification and strong winds create deep mixed layers (Mitchell et al., 1991; De Baar et al., 2005). Wind-induced vertical mixing reduces the total irradiance dose but periodically exposes phytoplankton cells to periods of excessive irradiance when residing near the surface (Denman and Gargett, 1983; Neale et al., 2003; Ross et al., 2008). These dynamic alterations

between low and high irradiance require regulation and photoacclimation of light harvesting, photosynthesis and photoprotective pigments. In response to low irradiance, algae maximize their light harvesting capacity and photosynthetic efficiency, while at saturating irradiance, the Calvin cycle activity increases at the expense of light harvesting pigments (Falkowski and La Roche, 1991). However, rapid irradiance fluctuations impose challenges to the photoregulation and photoacclimation processes, because high light conditions cause photodamage (Villafañe et al., 2003).

Recently, we showed that photodamage incurred by phytoplankton during the high light part of the light cycle induced by vertical mixing may be a factor controlling phytoplankton growth in regions with a deep upper mixed layer (UML) (Alderkamp et al., 2010). In the deep UML of the ACC, phytoplankton biomass was lower than in the shallow UML of the continental shelf, despite levels of both iron and average light in the UML being higher in the ACC. However, when phytoplankton growing in the UML of the ACC were exposed to surface irradiance levels, their photosystems were damaged considerably, most notably the D1 core protein of PS II (Bouchard et al., 2005a, 2005b; Alderkamp et al., 2010; Van de Poll et al., 2011). This negatively affected their growth rates, since damaged photosystems prevent efficient usage of the available light and the need

* Corresponding author at: Department of Environmental Earth System Science, Stanford University, Stanford, CA 94305, USA.
E-mail address: Alderkamp@Stanford.edu (A.-C. Alderkamp).

for repair increases metabolic costs (Kana et al., 2002; Dimier et al., 2009a). Thus, phytoplankton growth rates in deep UMLs are not only reduced by low mean irradiance levels, but they can also be reduced by photoinhibition as phytoplankton mix from depth up into well-lit surface waters.

Overall, the ability of phytoplankton to withstand excessive irradiance is strongly influenced by their capacity for photoacclimation, which involves changes in cellular pigment composition and protein turnover rates (Geider et al., 1993; Shelly et al., 2003; Van de Poll et al., 2005) and takes place on time scales of minutes to days (Falkowski and La Roche, 1991). An important protection mechanism against photodamage is the thermal dissipation of excess energy by xanthophyll cycle pigments in their de-epoxidated state. The xanthophyll cycle of algae comprises enzymatic conversion of carotenoids such as violaxanthin to antheraxanthin and zeaxanthin in green algae, and diadinoxanthin (dd) to diatoxanthin (dt) in diatoms and picoeukaryotic algae (Demmig-Adams, 1990; Olaizola et al., 1994; Olaizola and Yamamoto, 1994; Dimier et al., 2009a). The thermal dissipation of excess energy absorbed in PS II under high irradiance conditions can be quantified in vivo by estimating non-photochemical quenching (NPQ) of chlorophyll a (Chl a) fluorescence (Demmig et al., 1987; Demmig-Adams, 1990; Demmig-Adams and Adams, 2006). More specifically, the quenching of Chl a that is fast relaxing on a scale of seconds to minutes (qE) is related to thermal dissipation, which is mainly regulated by the $\Delta$pH of the thylakoid membrane. The quenching that relaxes on a time scale of minutes to hours is related to photoinhibition (qI) (Walters and Horton, 1991, Demmig-Adams et al., 1995, Maxwell and Johnson, 2000, Van de Poll et al., 2011).

Cellular xanthophyll cycle pigment content and the ratio of xanthophyll cycle pigments to photosynthetic pigments in phytoplankton may determine their resistance to excessive irradiance exposure (Van de Poll et al., 2006, 2007, 2011). Photoacclimation via xanthophyll cycle photoprotection depends on two enzymatic processes, de-epoxidation of dd to dt and de novo synthesis of xanthophyll cycle pigments. Directly following an increase in light intensity, de-epoxidation is a rapid process (seconds) that follows first order kinetics during the first two minutes, followed by linear de novo xanthophyll cycle pigment synthesis during the next 20–30 min (Olaizola and Yamamoto, 1994; Lavaud et al., 2004). In studies of both temperate and polar phytoplankton species,

increased ratios of xanthophyll cycle pigments to Chl a were related to increased photoprotection against excessive irradiance and UV exposure (Van de Poll et al., 2006, 2007, 2011; Dimier et al., 2009b).

When phytoplankton cells were cultured under fluctuating irradiance, de-epoxidation of xanthophyll cycle pigments is often observed during the irradiance maximum of a light cycle (Van Leeuwe et al., 2005; Van de Poll et al., 2007, 2009; Van Leeuwe and Stefels, 2007; Kropuenske et al., 2009). However, it is unknown to what extent xanthophyll cycle pigment synthesis on timescales of vertical mixing contributes to photoprotection. Moreover, the high winds associated with the deep UML in the ACC lead to rapid vertical mixing rates (Denman and Gargett, 1983; Cisewski et al., 2005; Croot et al., 2007) that may exceed rates of photoacclimation (Cullen and Lewis, 1988).

In the present study, we determined if natural phytoplankton populations in the Drake Passage are able to alter their ratio of xanthophyll cycle pigment to Chl a on the time scales of vertical mixing. Subsequently, we determined if short-term (hours) photoacclimation processes such as xanthophyll cycle pigment synthesis, increased the photoprotection against excessive irradiance exposure. This study presents field data confirming photoacclimation mechanisms previously observed in laboratory studies and provides ecological context of photoacclimation mechanisms employed by phytoplankton in deep wind driven UMLs of HNLC regions.

## 2. Methods

### 2.1. In situ sampling

This study was conducted during the last 17 days of the ANT XXIV/3 expedition onboard the R.V. Polarstern (31 March–16 April 2008) along a transect though the Drake Passage (Fig. 1, Table 1). Meteorological parameters were collected by the shipboard weather observatory and archived by the Polarstern Data System (PODAS). Total surface downwelling irradiance was recorded continuously and converted to photosynthetically available radiation (PAR). Wind speeds were measured by an anemometer attached to the ship mast at a height of 37 m and adjusted to a reference height of 10 m following Hsu et al. (1994). Hydrographic data at 31 stations were
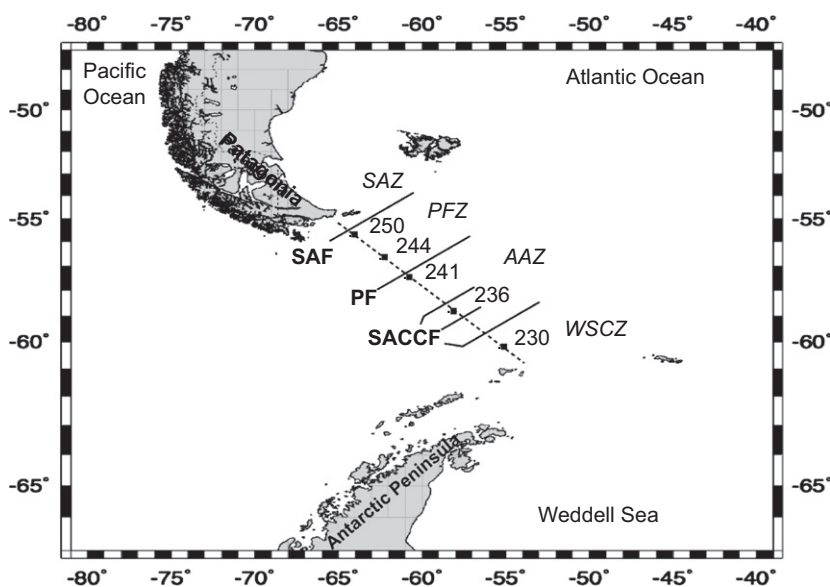


**Fig. 1.** Map showing the transect through the Drake Passage, including the locations of the experimental stations and the oceanic fronts (Provost et al., unpublished data). Abbreviations in alphabetical order: AAZ: Antarctic Zone, SACCF: Southern Antarctic Circumpolar Current Front, SAF: Subantarctic Front, SAZ: Subantarctic Zone, CZ: Continental Zone, PF: Polar Front. The Antarctic Circumpolar Current (ACC) flows eastward and is bounded to the north by the SAF and to the south by the most southern branch of the SACCF, which separates the WSCZ and the AAZ.

**Table 1**
Overview of supporting data of the experimental stations in the Drake Passage, the full set of nutrient data will be published in Middag et al. (submitted), the dFe data in Klunder et al. (unpublished).

| Station | Date | Position Lat. | Position Lon. | $z_{UML}$ | $NO_x$ ($\mu$mol L$^{-1}$) | $PO_4$ ($\mu$mol L$^{-1}$) | Si ($\mu$mol L$^{-1}$) | dFe (nmol L$^{-1}$) | Water temp. (°C) | Daily PAR (mol photons m$^{-2}$ day$^{-1}$) |
|---|---|---|---|---|---|---|---|---|---|---|
| 230 | 2 and 3-Apr | 60°6.23′S | 55°16.75′W | 42 | 27.1 | 1.9 | 54.6 | 0.77 | 1.3 | 7.6 and 4.6 |
| 236 | 5-Apr | 58°57.81′S | 58°5.81′W | 82 | 26.6 | 1.9 | 39.0 | 0.12 | 2.5 | 9.9 |
| 241 | 7-Apr | 57°37.33′S | 60°53.87′W | 74 | 25.4 | 1.7 | 8.9 | 0.26 | 3.0 | 6.3 |
| 244 | 9-Apr | 56°55.15′S | 62°22.73′W | 94 | 22.3 | 1.6 | 3.8 | 0.13 | 5.4 | 16.2 |
| 250 | 11-Apr | 55°44.15′S | 64°22.33′W | 108 | 23.2 | 1.6 | 4.2 | 0.38 | 5.1 | 9.2 |

collected using Seabird 911+ conductivity, temperature, depth (CTD) sensor and a Dr. Haardt fluorescence sensor. The depth of the upper mixed layer ($z_{UML}$) was calculated from each CTD profile as the shallowest depth at which the density ($\sigma_t$) was 0.02 kg m$^{-3}$ greater than at the surface. Water samples from discrete depths at 29 stations were obtained from Niskin bottles.

The attenuation of PAR in the water column was calculated using an empirical relationship between the diffuse attenuation coefficient of underwater light $K_d$[PAR] and the Chl $a$ concentration in the Southern Ocean at Chl $a$ concentrations between 0.05 and 14 mg m$^{-3}$ (Venables and Moore, 2010)

$$K_d[\text{PAR}] = 0.05 + 0.057[\text{Chl } a]^{0.58} \tag{1}$$

where [Chl $a$] is the mean Chl $a$ concentration (mg m$^{-3}$) of the surface 50 m measured by HPLC analysis (see below). The estimates of $K_d$[PAR] thus derived were similar to those estimated from satellite data in the center of the Drake Passage. $K_d$ was used to calculate the depths of the euphotic zone ($z_{EU}$) and total daily PAR within the UML ($E_{UML}$) as described in Alderkamp et al. (2010).

### 2.2. Pigments

At ambient seawater temperature, we filtered 0.9–2.5 L of seawater through a GF/F (Whatman) filter which was immediately flash frozen in liquid nitrogen and stored at −80 °C until analysis. Analysis of *in situ* samples was provided by the CNRS Laboratoire d'Etudes en Géophysique et Océanographie Spatiales, Toulouse, France. Filters were freeze-dried and extracted in 3 mL 100% methanol, disrupted by sonication and clarified by filtration through a GF/F filter (Whatman). The extracts were analyzed on a high performance liquid chromatography (HPLC) Agilent Technologies system, following Ras et al. (2008). The total Chl $a$ concentration varied by 2.3% between replicate samples. The pigments of experimental samples were analyzed separately at the Department of Ocean Ecosystems, University of Groningen, the Netherlands. For analysis of pigments, filters were freeze-dried (48 h) and extracted in 90% acetone (48 h). Pigments were separated on a HPLC Waters 2690 system (including a DeltaPakµmodule, 996 photodiode array detector) using a C18 reverse-phase column (Van Leeuwe et al., 2006). The total Chl $a$ concentration between replicate samples varied by less than 4.1%. On three stations, samples obtained from different casts on the same station were analyzed by both methods, with Chl $a$ concentrations varying by less than 10%.

The phytoplankton community composition at each station was derived from diagnostic pigments following Uitz et al. (2006).

### 2.3. Chlorophyll fluorescence parameters

The maximum quantum yield of photosystem II ($F_v/F_m$) (Krause and Weis, 1991) was determined at ambient seawater temperature with a pulse-amplitude modulated (PAM) fluorometer (WATER-PAM, Walz) and WinControl Software (Heinz Walz GmbH) on samples that were kept in the dark for at least 30 min at ambient temperature. When the measuring light (non-photochemistry inducing) of the PAM-fluorometer was turned on, the minimum fluorescence ($F_o$) of the sample was measured. The maximum fluorescence ($F_m$) was then measured by applying a saturating light pulse of 4000 µmol photons m$^{-2}$ s$^{-1}$ for 0.8 ms to close all PS II reaction centers. $F_v/F_m$ was calculated as

$$F_v/F_m = \frac{F_m - F_o}{F_m} \tag{2}$$

Seawater from each station was filtered through a GF/F and used to blank the PAM-fluorometer before measurements were made. By using unconcentrated samples from regions with low phytoplankton biomass for our analysis, the fluorescence levels were close to the detection limit of the PAM fluorometer. Although this resulted in significant variations in the fluorescence $F_o$ baseline under the measuring light, reproducibility of $F_v/F_m$ was always within 0.05 in triplicate measurements. Longer dark acclimation times (up to 45 min) did not increase the $F_v/F_m$ values.

### 2.4. Experiments

At five stations representing different hydrographic conditions (Figs. 1 and 3), phytoplankton samples were obtained from both a nighttime CTD cast and a daytime CTD cast. Samples were analyzed for $F_v/F_m$ and pigment concentration as described above and used for two different types of experiments (Fig. 2). During the nighttime cast, samples were obtained from the depth where light was 2% of surface values (calculated from the measured diffuse attenuation coefficient, $K_d$) and then incubated at either high (H) or low (L) irradiance for six hours (see high and low incubation experiments section) to study the xanthophyll pigment synthesis and photoacclimation processes. Following the 6-h incubation, samples from the H and L treatment were exposed to surface irradiance for 20 min (see short-term surface irradiance exposure [SIE] experiments) to assess their susceptibility to photodamage. From the daytime cast, samples were obtained from surface (S) and D waters (D, equivalent to approximately 2% of surface irradiance, Table 1). The susceptibility to photodamage by these populations upon exposure to excessive irradiance was tested in short-term SIE experiments.

#### 2.4.1. High and low irradiance incubation experiments

Triplicate samples were incubated in deck incubators at *in situ* water temperature in 1 L polycarbonate bottles under two different irradiance levels for six hours starting shortly after sunrise. The bottles were shaded by neutral density screening to achieve either high irradiance (H-treatment—50% of incident surface irradiance) or low irradiance (L-treatment—2% of incident surface irradiance) (Table 2). UVB radiation is fully and UVA radiation is partially blocked by the polycarbonate bottles (Van Donk, 2001). After the incubation, each bottle was analyzed for $F_v/F_m$ and pigment concentration. Subsequently, samples from each treatment were pooled and exposed to excessive irradiance in the SIE experiment (see below).

### 2.4.2. Short-term surface irradiance exposure (SIE) experiments

The sensitivity to excessive irradiance exposure of H and L samples and of S and D samples was tested in SIE experiments as described by Alderkamp et al. (2010). Briefly, phytoplankton cells were exposed to near-surface irradiance conditions (Table 2) for 20 min while floating at the surface of a deck incubator at *in situ* water temperature in 50 mL polystyrene culture flasks (Becton
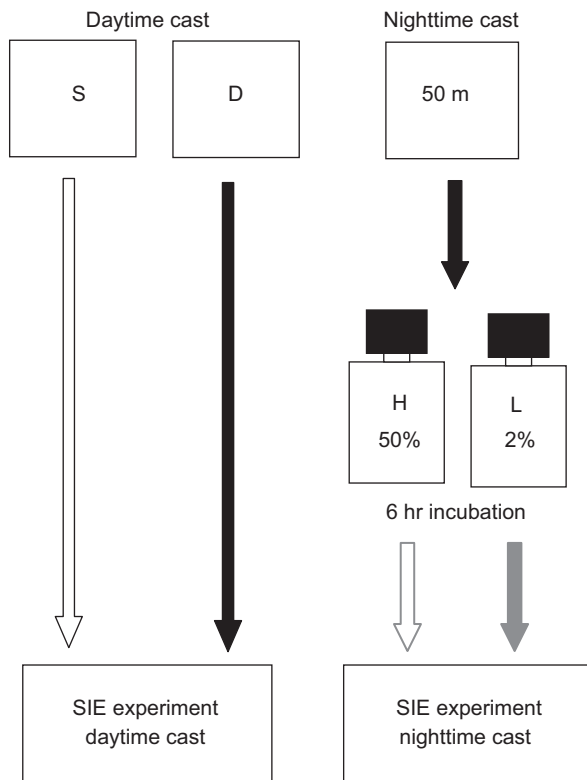


**Fig. 2.** Schematic illustration of the different incubation and exposure treatments performed at each station. Samples from the daytime cast were used to test the effect of photoacclimation processes within the water column on the susceptibility to photodamage in short-term (20 min) surface irradiance exposure (SIE) experiments. Samples were obtained from the surface (S) and subsurface (D) from a daytime cast and exposed to 20 min of surface irradiance in the absence or presence (+) of lincomycin, an inhibitor of repair of photosystem II. Samples from the nighttime cast were used to test the effects of photoacclimation processes during six hour incubation at 50% (H) or 2% (L) of incident irradiance on the susceptibility to photodamage in the SIE experiments described above.

Dickinson). The polystyrene flasks were transparent to both PAR and ultraviolet A (UVA), whereas UVB was blocked, which was confirmed by measuring absorption of the wall of the flask between 200 and 800 nm on a Perkin–Elmer Lambda 35 spectrophotometer. After 20 min, subsamples were removed and $F_v/F_m$ was determined after dark acclimation for 5 min. This allowed us to resolve the fast ($qE$) and slow ($qI$) relaxing components of total quenching ($qN$) (Alderkamp et al., 2010). Samples were then kept at low light (2 μmol photons m$^{-2}$ s$^{-1}$) under cool white fluorescent lamps at ambient seawater temperature to monitor recovery. Recovery of $F_v/F_m$ was followed for two hours at time intervals of approximately 30 min after 5 min of dark acclimation prior to each measurement. Two treatments were tested, the first with no addition of inhibitors and the second with the addition of $0.6 \times 10^{-3}$ mol L$^{-1}$ (final concentration) of lincomycin (Sigma, from a $100 \times$ stock solution freshly prepared in 96% of EtOH). Lincomycin inhibits transcription of chloroplast-encoded proteins such as the D1 reaction center protein (Bouchard et al., 2005a). Lincomycin was added 10 min before the start of the SIE to ensure sufficient time for uptake by phytoplankton cells. Experiments were carried out in triplicate and a single control sample for each treatment was not exposed but kept at ambient seawater temperature and low light conditions (2 μmol photons m$^{-2}$ s$^{-1}$) as measured by a Biospherical Instruments QSL Quantum Scalar Laboratory Sensor (Biospherical Instruments Inc., San Diego, CA, USA).

The SIE experiments were designed to study the exposure of phytoplankton communities to irradiance conditions in the upper water column. Measurements of surface irradiance during the cruise revealed maximum PAR levels during the day of > 800 μmol photons m$^{-2}$ s$^{-1}$, averaging 620 μmol photons m$^{-2}$ s$^{-1}$ over the Drake Passage transect. The mean irradiance during the exposure experiments was 235 μmol photons m$^{-2}$ s$^{-1}$ (Table 2), which is equivalent to 38% of the mean daily irradiance maximum. The 38% surface irradiance level in the water column corresponded to a depth of 13.1 m, taking the mean $K_d$ of all stations into account. Thus, the irradiance levels in the surface irradiance exposure experiments are lower than those experienced by phytoplankton in the upper 13 m of the water column during the average maximum irradiance levels of the day. Consequently, phytoplankton cells that are mixed up to the upper few meters of the water column may experience higher irradiance levels and thus more photodamage than in our surface irradiance exposure experiments.

Standard trace metal clean (TMC) procedures were not followed during the experiments, but contamination with trace metals is unlikely to have an effect, given the short time frame of the incubations. Values of $F_v/F_m$ often display the first response to

**Table 2**
Overview of initial data and PAR levels during short-term surface irradiance exposure experiments.

| Station | Nighttime cast | | | | | Daytime cast | | | | |
|---|---|---|---|---|---|---|---|---|---|---|
| | Sample depth | $F_v/F_m$ | (dd+dt): Chl a | PAR incubation (μmol photons m$^{-2}$ s$^{-1}$) | PAR SIE (μmol photons m$^{-2}$ s$^{-1}$) | Time after sunrise (hh:mm) | Sample depth (S) (D) | $F_v/F_m$ | (dd+dt): Chl a | PAR SIE (μmol photons m$^{-2}$ s$^{-1}$) |
| 230 | 50 | 0.567 | 0.058 | 115 (8–408) | 258 (180–279) | 05:20 | 5 | 0.486 | 0.114 | 166 (131–203) |
| | | | | | | | 65 | 0.598 | 0.051 | |
| 236 | [a] | [a] | [a] | 391 (193–781) | 339 (270–406) | 00:10 | 5 | 0.417 | 0.071 | 294 (271–316) |
| | | | | | | | 60 | 0.414 | 0.070 | |
| 241 | 50 | 0.308 | 0.064 | 210 (99–361) | 137 (91–197) | 01:50 | 25 | 0.273 | 0.123 | 293 (226–361) |
| | | | | | | | 75 | 0.373 | 0.070 | |
| 244 | 50 | 0.418 | 0.072 | 582 (165–1036) | 119 (91–138) | 03:50 | 5 | 0.047 | 0.085 | 604 (498–671) |
| | | | | | | | 60 | 0.281 | 0.077 | |
| 250 | 50 | 0.276 | 0.108 | 350 (54–575) | 161 (133–195) | 02:55 | 25 | 0.193 | 0.124 | 344 (281–369) |
| | | | | | | | 75 | 0.219 | 0.107 | |

[a] Only one cast was deployed shortly after sunrise for station 236. The subsurface sample was used for the six hour incubation as well as the surface irradiance exposure experiment.

additions of trace metals in HNLC regions and it takes several hours to days to observe a response (Behrenfeld et al., 1996; Boyd et al., 2000). No increase in $F_v/F_m$ was observed in the control samples of the short-term surface irradiance exposure experiments.

### 2.5. Statistics

The initial response of the phytoplankton $F_v/F_m$ after surface irradiance exposure was tested using a one-way ANOVA, followed by a post-hoc Tukey test. The recovery was assessed using repeated measures of ANOVA with the Statistica software (release 7,

StatSoft Inc.). Relationships between surface parameters were tested using simple linear regression analysis.

## 3. Results

### 3.1. Hydrographic setting, chlorophyll distribution, and phytoplankton chemotaxonomy

The transect through the Drake Passage traversed three systems from south to north (Fig. 1): the Southern Antarctic Circumpolar
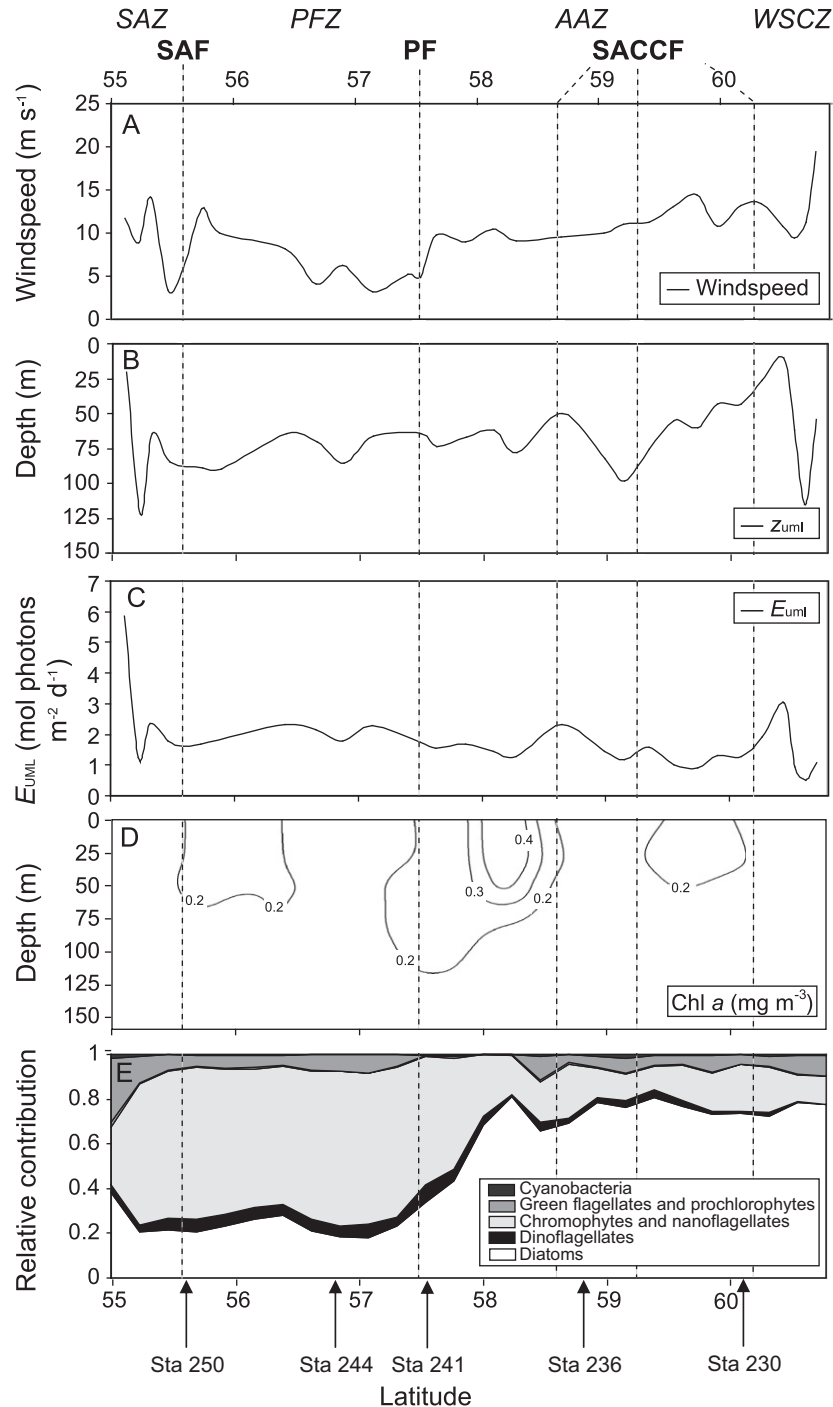


**Fig. 3.** Section graphs of the Drake Passage transect; data are interpolated between stations. The location of the fronts encountered in austral fall 2008 and the oceanic zones are indicated above the figure, the location of the experimental stations below; abbreviations as in Fig. 1. (A) The mean wind speed over one hour prior to finishing the cast. (B) The depth of the upper mixed layer ($z_{UML}$). (C) The mean daily irradiance available to phytoplankton in the UML ($E_{UML}$). (D) Fluorescence scaled to Chl $a$ concentration in mg m$^{-3}$. (E) Mean phytoplankton species composition of the upper 50 m derived from the pigment composition as per Uitz et al. (2006).

Current Front (SACCF) which contained three branches (at 60°20S, 59°20S, and 58°40S), the Polar Front (PF) at 57°30S, and the Subantarctic Front (SAF) at 55°40S (Provost et al., unpublished data). Surface water concentrations of nitrate and phosphate were high and constant across the whole Drake Passage transect ($> 22$ and $> 1.5 \mu$mol $L^{-1}$, respectively, Table 1), whereas the concentrations of silicate and iron differed between oceanic regions bordered by frontal systems. South of the most southern branch of the SACCF, in the Weddell Scotia Confluence Zone (WSCS), surface waters are influenced by Weddell Sea Shelf Water (WSSW) from the eastern shelf of the Antarctic Peninsula (Whitworth et al., 1994; Hofmann et al., 1996; Amos, 2001). This water was colder (mean $-0.25$ °C) and more saline ($> 34$) than surface waters in the ACC, and is rich in iron ($> 0.8$ nmol $L^{-1}$) and silicate ($> 76 \mu$mol $L^{-1}$) (Table 1). North of this branch, in the Antarctic Zone (AAZ), the surface waters of the ACC are composed of Antarctic Surface Water (AASW). The branches of the SACCF formed mesoscale eddies that were visible in the temperature transect and satellite images (results not shown). The upper AASW was warm (2–4 °C) and relatively fresh (salinity $\sim 33.8$), and contained low iron concentrations ($< 0.3$ nmol $L^{-1}$). Silicate concentrations were somewhat lower than those found in the surface waters of the WSCS, but still relatively high ($> 10 \mu$mol $L^{-1}$) (Table 1). Along the transect, the PF was located at 57°30S. North of the PF, in the Polar Frontal zone (PFZ), concentrations of silicate and iron in the UML were generally low (mean 4 and 0.3 $\mu$mol $L^{-1}$, respectively, Table 1). North of the SAF, near-coastal waters were warmer than waters in the PFZ (mean 6.2 °C), were low in silicate ($< 3.8 \mu$mol $L^{-1}$), and contained more iron than waters in the PFZ (Table 1).

The mean wind speed while on station was moderate throughout the Drake Passage (Fig. 3A), while episodes of higher winds were observed while in transit (results not shown). The highest wind speeds were measured close to the Antarctic Peninsula and the lowest around the PF. In general, moderate to high winds translated into a deep UML over the whole Drake Passage transect, with a few exceptions (Fig. 3B).

Levels of surface PAR were low close to the Antarctic Peninsula due to extensive cloud cover. This was observed in the eight-day composites of SeaWiFS satellite data, as well as onboard observations (data not shown). The low surface PAR and relatively deep $z_{UML}$ resulted in low mean levels of PAR in the UML ($E_{UML}$, $< 1$ mol photons $m^{-2}$ $d^{-1}$, Fig. 3C). Further north, the cloud cover was reduced and PAR was higher, resulting in a slightly higher $E_{UML}$ ($\sim 2$ mol photons $m^{-2}$ $d^{-1}$).

Phytoplankton biomass was low throughout surface waters of the Drake Passage (mean 0.2 mg Chl $a$ $m^{-3}$ throughout the upper 50 m), except for the region of the AAZ between 58°17.81′S and 58°5.92′S, where surface Chl $a$ concentrations were higher (Fig. 3D). The higher biomass in this region was associated with an eddy, which can enhance conditions for phytoplankton growth (Kahru et al., 2007). In addition, phytoplankton in this area was possibly influenced by Fe input during a recent dust deposition event (M. Klunder, pers. com.). The phytoplankton community composition roughly followed the trends in macronutrient concentrations. Diatoms dominated south of the PF where silicate concentrations were high. North of the PF, nanoflagellates and chromophytes dominated the phytoplankton community with diatoms still contributing significantly (Fig. 3E).

## 3.2. Ratios of xanthophyll cycle pigments (dd+dt) to Chl a

Surface ratios of xanthophyll cycle pigments (dd+dt):Chl $a$ varied between 0.12 and 0.23 across the Drake Passage, with no significant differences between oceanic regions (one-way ANOVA, $p > 0.05$). Dt was not detected in the samples from the Drake Passage, indicating that all dt had been epoxidated to dd, a process that takes several minutes at low light (Van de Poll et al., 2006; Kropuenske et al., 2010). Since an unknown fraction of the xanthophyll cycle pigments will be present as dt in the field, all ratios are presented as (dd+dt):Chl $a$. Throughout the Drake Passage transect, (dd+dt):Chl $a$ was highest at the surface (Fig. 4), with large decrease in this ratio observed below the $z_{UML}$ (Fig. 4). A decreasing gradient in this ratio with depth was also observed within the UML, indicative of pigment synthesis by phytoplankton within the UML. The largest vertical gradients of the (dd+dt):Chl $a$ ratio within the UML were found in stations with low wind speeds close to the PF (Fig. 4A, B).

## 3.3. Fluorescence characteristics

The highest $F_v/F_m$ values were measured in samples of the southernmost station 230 (Table 2), where the phytoplankton biomass was dominated by diatoms. At this station, the water column was influenced by iron-rich WSSW water, and both in situ PAR and $E_{UML}$ were low (Table 1, Fig. 3C). The $F_v/F_m$ values decreased with latitude to the north over the Drake Passage transect. The lowest $F_v/F_m$ values were measured in surface samples of the daytime cast at the northernmost stations 244 and 250. These stations were dominated by chromophytes and nanoflagellates and concentrations of silicate and iron were low, whereas in situ PAR and $E_{UML}$ were moderate to high.
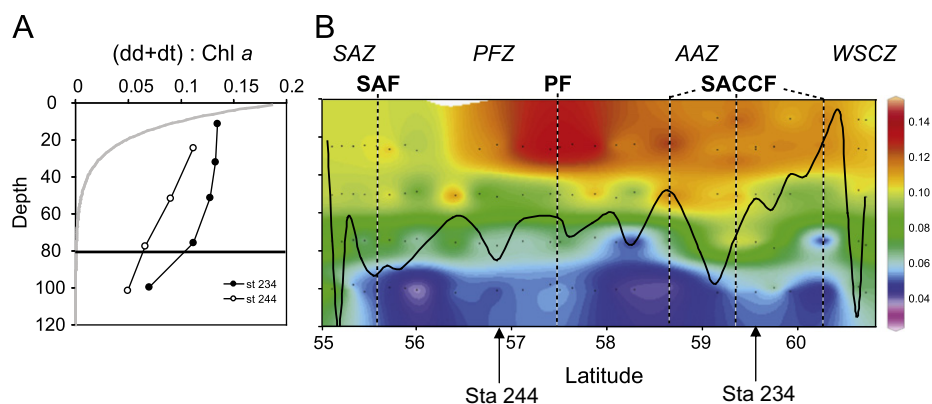


**Fig. 4.** (A) Section graph of the ratio of xanthophyll cycle pigments (dd+dt) to Chl $a$ (mol:mol). The location of the fronts encountered in austral fall 2008 are indicated above the figure, abbreviations as in Fig. 1. The black line indicates the depth of the UML as in Fig. 3B. (B) Comparison of (dd+dt):Chl $a$ ratios over depth at station 234 with a high wind speed (11.3 m s$^{-1}$) and station 244 wind a low wind speed (3.6 m s$^{-1}$). The light attenuation was similar for these stations and the percentage of surface PAR is depicted by a gray line. The mean $z_{UML}$ of the two stations is depicted by a black line (75 m for station 234, 86 m for station 244).

On all stations, surface samples from the daytime cast showed signs of photoacclimation to higher light levels, displaying lower values of $F_v/F_m$ and higher (dd+dt):Chl $a$ ratios when compared to the subsurface sample (Table 2).

### 3.4. High and low irradiance incubation experiments

To study the photoacclimation of phytoplankton to surface and subsurface irradiance levels, phytoplankton samples obtained from the subsurface before sunrise were incubated at one of the two different irradiance levels that simulated either surface irradiance (H; 50% of in situ irradiance) or irradiance at the base of the mixed layer (L; 2% of surface irradiance, equivalent to ~60 m depth). The different experimental stations were situated in different water masses (Fig. 1) and were dominated by different phytoplankton groups (Fig. 3E). In addition, PAR$_{surf}$ during the incubations varied greatly between the different experimental days (Table 2). Nevertheless, the effect of the H and L incubations on $F_v/F_m$ and the (dd+dt):Chl $a$ ratio of the phytoplankton communities was remarkably similar. The $F_v/F_m$ was mostly unaffected by the L treatment, except for station 230, where a small increase was observed (Fig. 5A). In the H treatment, $F_v/F_m$ decreased significantly in all stations by an average of 56% when compared to the initial values. Similarly, (dd+dt):Chl $a$ was mostly unaffected by the L treatment, except for station 230 where a small increase was observed (Fig. 5B). In the H treatment, (dd+dt):Chl $a$ increased on an average of 38%. The strongest and weakest increases were observed at station 230 and 236, respectively, the two southernmost stations. It is unlikely that the changes in (dd+dt):Chl $a$ were caused by changes in cellular Chl $a$, since ratios of but, fuc and hex to Chl $a$ were unaffected (results not shown).
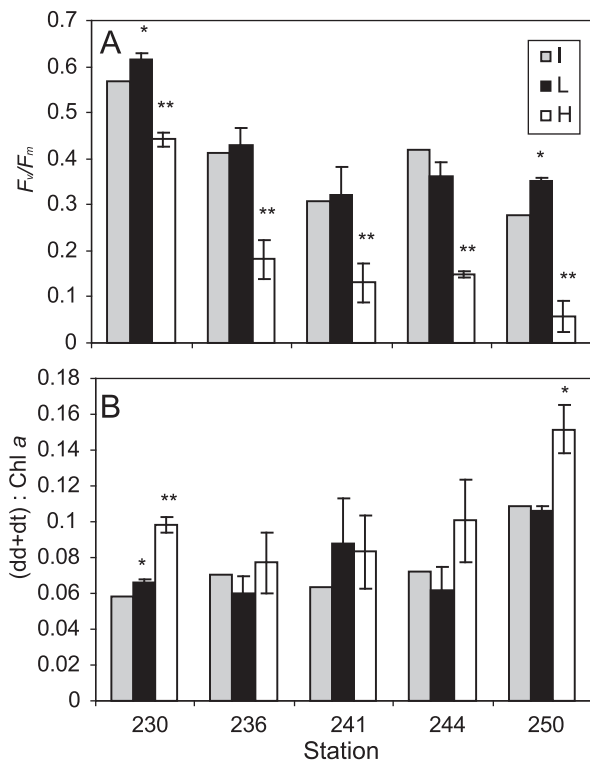


**Fig. 5.** Results of the six-hour phytoplankton incubations under high irradiance (H) and low irradiance (L) conditions. (A) $F_v/F_m$ (B) ratio of xanthophyll pigments (dd+dt) to Chl $a$. Significant differences (one-way ANOVA) from initial values are indicated with asterisks; $^*p < 0.05$, $^{**}p < 0.01$.

### 3.5. Short-term surface irradiance exposure (SIE) experiments

#### 3.5.1. Daytime cast

Exposure of phytoplankton samples obtained from the surface and the subsurface during the daytime cast to near-surface irradiance conditions (Table 2) for 20 min caused a strong reduction in the $F_v/F_m$ in all experimental treatments for each station (Fig. 6, left panels) resulting in a mean $qN$ of 0.68 (SD 0.22). In each experiment, a control sample that was not exposed to surface irradiance but was kept at the low irradiance used for recovery showed no change in $F_v/F_m$ over the 140 min duration of the experiment (results not shown). Results from the SIE experiment at station 244 are not shown since the fluorescence signal was below the detection limit of the PAM-fluorometer.

The $F_v/F_m$ recovered when cells were subsequently shifted to low irradiance in all experiments (Fig. 6, left panels). The rapid recovery during the first 30 min after surface irradiance exposure related to fast relaxing energy-dependent quenching resulted in a mean $qE$ of 0.22 (SD 0.14). The slow recovery of $F_v/F_m$ related to photoinhibitory quenching resulted in a mean $qI$ of 0.46 (SD 0.31). In all experiments, the recovery was negatively affected by blocking the repair of the D1 protein by addition of lincomycin, although the effect was significant in the experiments at stations 241 and 250 only.

A small effect of sampling depth on the recovery of $F_v/F_m$ was apparent at stations 230 and 241. These were the stations where the D sample was obtained from below $z_{UML}$ (Table 1). In the other stations, both the S and D sample were obtained within the UML and there was no effect of the sampling depth on the recovery of $F_v/F_m$. In the experiment at station 230, the sampling depth mainly affected the initial fluorescence quenching. The D samples showed a stronger initial quenching than the S samples, whereas the recovery was similar. In contrast, in the experiment on station 241, the initial quenching of D and S samples was similar, but there were differences in the recovery, particularly in the lincomycin treated samples.

#### 3.5.2. Nighttime cast SIE experiment after H and L incubation

To study the effects of the photoacclimation processes during the six hour incubation on the susceptibility to photodamage by excessive irradiance, H and L phytoplankton samples were subjected to SIE experiments. Similar to the experiments with the daytime casts, exposure of phytoplankton samples (Table 2) caused a reduction in $F_v/F_m$ values in all experiments (Fig. 6, right panels), resulting in a mean $qN$ of 0.76 (SD 0.19). The $F_v/F_m$ recovered during subsequent incubation at low irradiance, resulting in a mean $qE$ of 0.42 (SD 0.13) and a mean $qI$ of 0.35 (SD 0.18). Recovery from high light exposure was negatively affected by the addition of lincomycin, although the effect was not significant in the experiment at station 230. There were minor differences in recovery between samples derived from the H and L incubations, which were only significant in station 250, where recovery in L samples was faster than in H samples. Thus, despite an increased ratio of (dd+dt):Chl $a$ in the phytoplankton in H incubations (Fig. 5), there was no positive effect on the recovery after excessive irradiance exposure when compared to the L incubations.

## 4. Discussion

### 4.1. Xanthophyll cycle pigment synthesis in response to vertical mixing

The phytoplankton biomass was low across the Drake Passage in the austral fall of 2008. South of the PF, the phytoplankton
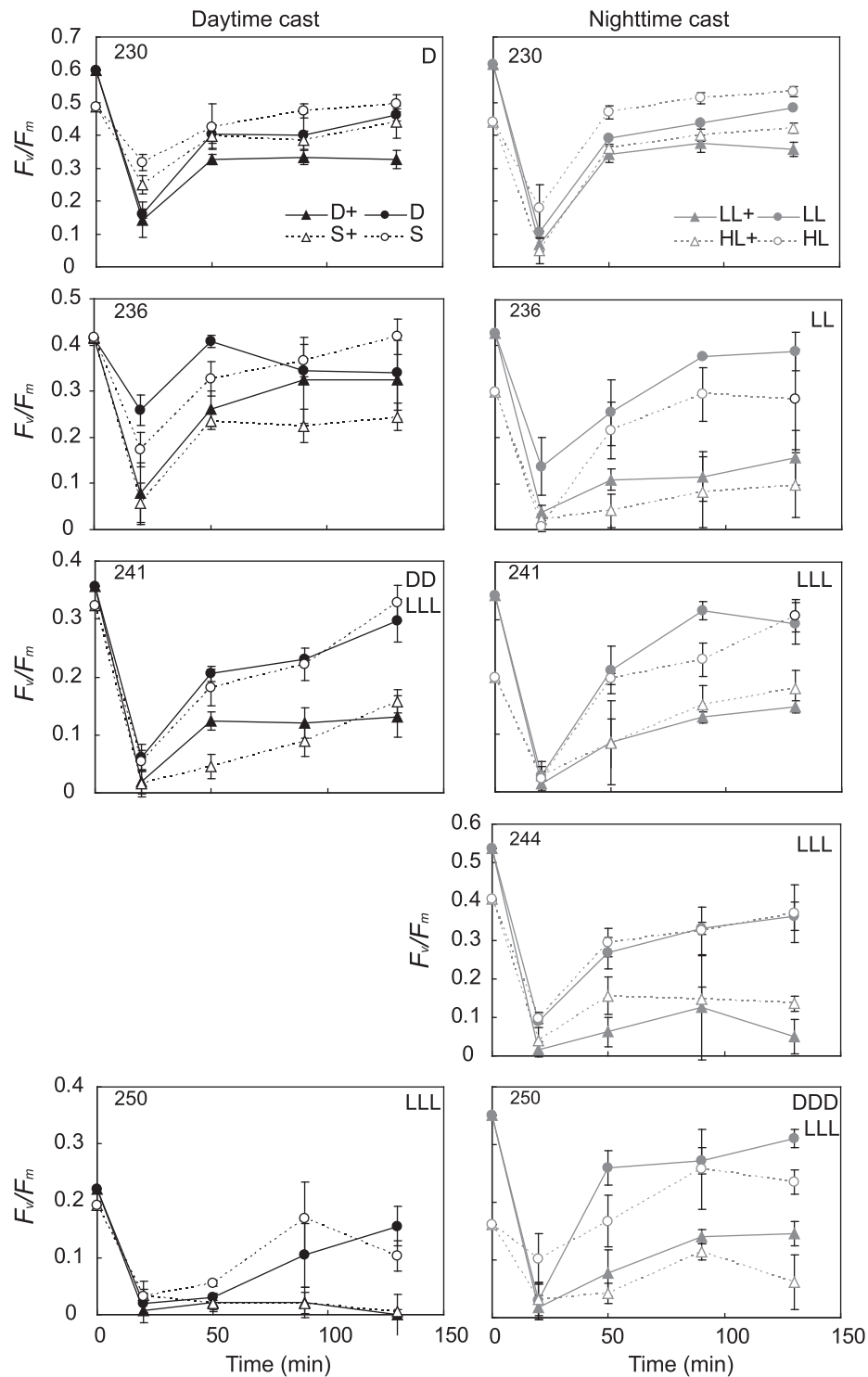
**Fig. 6.** Results of the short-term photoinhibition experiments with phytoplankton samples taken from the surface (S, 5–10 m depth) and the subsurface (D, 40–60 m depth) of the daytime cast (left) and from subsurface samples of the nighttime cast that were previously incubated for six hours under high irradiance (H) and low irradiance (L) (right). PS II efficiency ($F_v/F_m$) dynamics were measured after exposure to surface irradiance conditions for 20 min and subsequent recovery at low irradiance. Means and standards deviation are shown for three replicates of untreated phytoplankton samples and samples with the addition of lincomycin (+), an inhibitor of repair of the D1 core protein of PS II. Significant differences (repeated measures of ANOVA) between recovery characteristics samples with and without the addition of lincomycin are indicated with L: $p < 0.05$, LL: $p < 0.01$, LLL: $p < 0.001$, and of the S and D or H and L samples with D: $p < 0.05$, DD: $p < 0.01$, DDD: $p < 0.001$.

community was dominated by diatoms, whereas nanoflagellates and chromophytes were dominant north of the PF with diatoms still contributing significantly. A similar phytoplankton community structure across the Drake Passage was observed by Sosik and Olson (2002) in late summer. Generally, the PF separates the low Fe, high $NO_3$ waters in the south from the high Fe, low $NO_3$

waters in the north (Chisholm and Morel, 1991), which may lead to Fe-limitation of phytoplankton south of the PF (Sosik and Olson, 2002). However, we found high concentrations of $NO_3$ over the whole Drake Passage; whereas concentrations of dissolved Fe in surface waters were variable (Middag et al., submitted; Klunder et al., unpublished) and the high surface values of $F_v/F_m$ in the

stations south of the PF do not suggest physiological Fe limitation for phytoplankton in our study.

The rates of wind-driven vertical mixing in the UML of the open ocean may be high, particularly in regions with high wind speeds (Denman and Gargett, 1983; Cisewski et al., 2005). High vertical mixing rates in combination with a deep $z_{UML}$ that was present in most of the stations in the Drake Passage yield a light climate for phytoplankton cells of levels of $E_{uml}$ with short episodes of excessive irradiance exposure when residing at the surface. The surface ratios of (dd+dt):Chl $a$ resembled those of low-light acclimated phytoplankton cultures (Dimier et al., 2009b; Kropuenske et al., 2009) and were lower than those observed at the surface of stable water columns in coastal Antarctic waters in the Austral summer (Moline, 1998). The presence of a vertical gradient in (dd+dt):Chl $a$ within the UML shows that these low light acclimated phytoplankton constantly and rapidly adjust their (dd+dt):Chl $a$ ratio in response to changing irradiance conditions due to vertical mixing. Despite the significant changes in phytoplankton community composition with latitude, the vertical pigment gradient was observed in almost all stations in the Drake Passage. These included stations north of the PF that were dominated by nanoflagellates and chromophytes and stations south of the PF that were dominated by diatoms. Thus, throughout the phytoplankton community in the open ocean, xanthophyll cycle pigments are being synthesized *de novo* when phytoplankton cells are mixed up to high irradiance surface waters. Chl $a$ synthesis during downward vertical mixing also may have contributed to the gradient in (dd+dt):Chl $a$. However, photoacclimation to a decreasing light intensity generally takes longer than photoacclimation to a higher light intensity (MacIntyre et al., 2000; Lavaud et al., 2007) and hence, the contribution of Chl $a$ synthesis was likely small. Moreover, no increase in Chl $a$ with depth was observed in the profiles and the minimal increase in Chl $a$ concentrations in the incubation experiments after six hours under L conditions evidenced low Chl $a$ synthesis rates (results not shown).

The photoprotection through *NPQ* that is related to the thermal dissipation of excess energy absorbed by PS II is dependent on the presence of the de-epoxidated xanthophyll cycle pigment dt (Demmig-Adams, 1990; Olaizola et al., 1994; Olaizola and Yamamoto, 1994; Dimier et al., 2009a). We could not study the de-epoxidation of xanthophyll cycle pigments and did not observe any dt in our field samples because the time it took to sample and filter the large volumes of water with low biomass exceeded the time required for epoxidation of dt into dd under low light. When phytoplankton cells were subjected to an increase in irradiance, up to 80% of the xanthophyll cycle pigments were present as dt (Van de Poll et al., 2006, 2011; Kropuenske et al., 2010), indicating that most of the xanthophyll cycle pigment pool can be used for photoprotection. Oceanic diatom species, however, may have an impaired ability for *NPQ* via de-epoxidation of xanthophyll cycle pigments (Strzepek and Harrison, 2004; Lavaud et al., 2007). This is because their photosynthetic architecture has evolved to contain fewer Fe-rich components to reduce their Fe requirement in Fe-poor waters (Strzepek and Harrison, 2004). However, this has impaired their ability to generate the strong $\Delta$pH across the thylakoid membrane needed for de-epoxidation of dd. Consequently, they exhibit lower *NPQ* than coastal diatom species (Strzepek and Harrison, 2004; Lavaud et al., 2007). Nonetheless, the constant xanthophyll cycle pigment synthesis in the UML throughout the Drake Passage transect suggests that oceanic phytoplankton invest energy in xanthophyll cycle pigment synthesis. Therefore, xanthophyll cycling seems to be a significant mechanism for photoacclimation to rapid changes in irradiance in oceanic phytoplankton.

### 4.2. Estimated rates of xanthophyll cycle pigment synthesis

Our results showed that the vertical gradient of (dd+dt):Chl $a$ was related to wind speed (linear regression $n=23$, $R^2=0.39$, $p < 0.01$), based on stations with three or more data points within the UML. The strongest vertical gradients were observed at stations close to the PF, where wind speeds were low. Low wind speeds generate slow mixing, since the vertical mixing velocity within the UML scales with the wind speed (Pollard, 1973; Denman and Gargett, 1983; Cisewski et al., 2005). Under these conditions, rates of pigment synthesis can exceed mixing rates and cells can photoacclimate to *in situ* light levels. Under conditions of high wind speed and rapid vertical mixing, rates of pigment synthesis are slower than mixing rates and cells are unable to fully photoacclimate to *in situ* light levels (Falkowski, 1983; Cullen and Lewis, 1988).

The rate of xanthophyll cycle pigment synthesis is an important factor in determining the photoacclimation potential of phytoplankton (Olaizola and Yamamoto, 1994; Lavaud et al., 2004). Several studies have related changes in phytoplankton pigment composition to time scales and rates of vertical mixing (Falkowski, 1983; Bidigare et al., 1987; Cullen and Lewis, 1988; Moline, 1998; Brunet et al., 2008; Griffith et al., 2010). Therefore, to estimate *de novo* synthesis rates in the UML of the Drake Passage, the vertical mixing velocity ($u_t$) was calculated following Denman and Gargett (1983):

$$u_t = 2w^* \tag{3}$$

where $w^*$ is the turbulent friction velocity in m s$^{-1}$, calculated as

$$w^* = \sqrt{\tau/\rho_w} \tag{4}$$

where $\rho_w$ is the density of seawater ($1.025 \times 10^3$ kg m$^{-3}$), and $\tau$ is the wind stress, given by

$$\tau = \rho_a C_{10}(U_{10})^2 \tag{5}$$

where $\rho_a$ is the density of air (1.2 kg m$^{-3}$), $C_{10}$ is the drag coefficient ($1.3 \times 10^{-3}$), and $U_{10}$ is the mean wind speed 10 m above the sea surface (m s$^{-1}$), which was calculated from the wind speed obtained from the ship board weather station.

At a location with a relatively high wind speed (10 m s$^{-1}$), such as station 234 (Fig. 4B), $u_t$ is $2.5 \times 10^{-2}$ m s$^{-1}$. This means that upward vertical mixing takes the phytoplankton cells through a tenfold increase in irradiance in approximately 20 min. At stations with a relatively low wind speed (e.g., station 244, 4.9 m s$^{-1}$), $u_t$ is $8.3 \times 10^{-3}$ m s$^{-1}$ and upward vertical mixing takes the phytoplankton cells through a tenfold increase in irradiance levels in approximately one hour. These vertical velocities are somewhat higher than those reported for subantarctic waters with deep UMLs southeast of New Zealand (Griffith et al., 2010).

We used the values of $u_t$ calculated in this way and the gradient in (dd+dt):Chl $a$ over the depth of the UML, to estimate the *de novo* synthesis rates of xanthophyll cycle pigments (Fig. 7). These estimated rates averaged 11.3 μmol dd+dt mol$^{-1}$ Chl $a$ s$^{-1}$, with a range of 0.9–25.0 μmol dd+dt mol$^{-1}$ Chl $a$ s$^{-1}$. These rates represent the mean over the time it takes for a cell to be transported from the bottom of the UML to the surface and vice versa, as the synthesis rate may vary with depth due to differences in irradiance. Rates did not differ significantly by oceanic region or dominant phytoplankton group (one-way ANOVA, $p > 0.05$). The variation in rates was greatest in the AAZ, which was also where branches in the SACCF and mesoscale eddies were observed. These features, together with wind speed, influence rates of vertical mixing (Kahru et al., 2007). The effect of eddy activity on vertical mixing speed may explain the poor correlation between the vertical gradient of (dd+dt):Chl $a$ and wind speed in
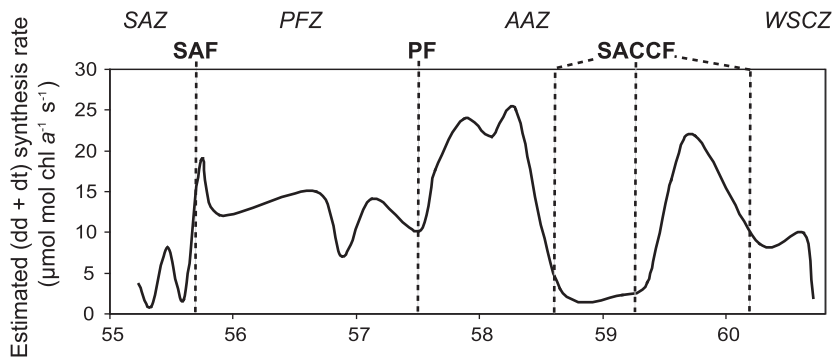
**Fig. 7.** Estimated rates of *in situ* xanthophyll cycle pigment synthesis within the UML over the Drake Passage transect, computed using vertical mixing velocities as per Denman and Gargett (1983) and the gradient of (dd+dt):Chl *a* within the UML presented in Fig. 3; see text for details.

the AAZ (linear regression, $n=10$, $R^2=0.12$, $p=0.33$). When stations in the AAZ were excluded from the regression analysis, the relationship between the gradient of (dd+dt):Chl *a* over depth and wind speed over the Drake Passage was stronger ($n=13$, $R^2=0.52$, $p<0.01$).

The estimates of these *in situ* photoprotection rates through pigment synthesis are in good agreement with the estimates of *de novo* xanthophyll cycle pigment synthesis rates in culture studies of temperate diatoms following a shift from low to high irradiance. Olaizola and Yamamoto (1994) measured a *de novo* xanthophyll cycle pigment synthesis rate of 31.8 μmol dd+dt mol$^{-1}$ Chl *a* s$^{-1}$ after shifting cultures of the diatom *Chaetoceros muelleri* to approximately threefold higher light intensities. Lavaud et al. (2004) reported *de novo* xanthophyll cycle pigment synthesis rates between 4.0 and 9.8 μmol dd+dt mol$^{-1}$ Chl *a* s$^{-1}$ for temperate diatoms, which varied between species, with light intensity, and with duration of light exposure. *De novo* xanthophyll cycle synthesis rates in the Antarctic diatom *Fragilariopsis cylindrus* were lower than those of the temperate diatoms. At 1.3 μmol dd+dt mol$^{-1}$ Chl *a* s$^{-1}$ over the first eight hours after a shift to 25-fold higher irradiance levels (Kropuenske et al., 2009, 2010), these rates are in the lower ranges of our *in situ* estimates, whereas the Antarctic haptophyte *Phaeocystis antarctica* did not show any significant xanthophyll synthesis after the shift to higher irradiance (Kropuenske et al., 2010). *P. antarctica* would be part of the nanoflagellates and chromophytes group south of the PF based on chemotaxonomy in our study and their spatial distribution (Schoemann et al., 2005). *De novo* xanthophyll cycle pigment synthesis rates in six temperate chromophyte species belonging to the pico- or nano-phytoplankton showed substantial variation between species and with light shift characteristics (Dimier et al., 2009b). Maximum rates of (dd+dt) synthesis during gradual increases in light levels ranged from 4.2 to 16.7 μmol dd+dt mol$^{-1}$ Chl *a* s$^{-1}$.

Low temperature negatively affects enzyme activity (Li et al., 1984), which impacts photosynthesis (Tilzer et al., 1986), respiration (Tilzer and Dubinsky, 1987), and growth rates (Sakshaug and Holm-Hansen, 1986) in phytoplankton in high latitude environments. However, no temperature effect was found on xanthophyll cycle pigment synthesis rates across the Drake Passage (linear regression, $n=23$, $R^2=0.01$, $p=0.76$). This suggests that phytoplankton in high latitude environments are adapted for rapid *de novo* xanthophyll cycle pigment synthesis rates, despite lower enzyme activity because of low temperatures.

Although vertical mixing within the UML is controlled primarily by wind stress (Pollard, 1973), over the Drake Passage, $z_{UML}$ at a given station was not correlated to the local wind speed (linear regression, $n=27$, $R^2=0.06$, $p=0.24$). The absence of such a relationship may be explained because the response time of $z_{UML}$ to wind forcing is on the order of several days (Cisewski et al., 2005). They found a significant relationship between wind speed and $z_{UML}$ only when the wind speed

was integrated over time scales of three inertial periods or longer, which in these latitudes, corresponds to several days. The wind speed depicted in Fig. 3A and used for calculations in our study was averaged over one hour prior to concluding the cast at each station. This time frame was chosen to approximate the average time scale for vertical movement around the UML (68 min, results not shown).

Additionally, the rate of xanthophyll cycle pigment synthesis was not related to $z_{UML}$ (linear regression, $n=23$, $R^2=0.01$, $p=0.66$). Similarly, there was no relation between xanthophyll de-epoxidation rates and $z_{UML}$ in the subantarctic open ocean (Griffith et al., 2010). An explanation may lie in the exponential decrease in irradiance with depth which causes the greatest gradients in light intensity at the top few meters of the water column (Fig. 4B). Thus, the time spent in transition from low light to high light that would trigger xanthophyll cycle pigment synthesis depends mostly on the vertical mixing speed at the very surface (and thus the wind speed), and deepening of the UML primarily increases the time a phytoplankton cell spends at low light levels.

### 4.3. The impact of short-term photoacclimation processes on prevention from photodamage

The results presented here show that photodamage was apparent in all surface irradiance exposure experiments despite vast differences in surface irradiance levels, water temperature, $z_{UML}$, and phytoplankton community composition. Even after exposure to relatively low irradiance levels (compared to the maximum irradiance levels during the day), photoinhibition was evidenced by both delayed recovery of $F_v/F_m$ (*qI*) and the negative impact of inhibiting the repair of the PS II D1 core protein by the addition of lincomycin. The slow relaxation of fluorescence quenching was not completely blocked by the addition of lincomycin in all short-term surface irradiance exposure experiments, most notably in the experiments from the nighttime cast on station 241 and 250. The slow relaxation in the lincomycin treated samples may have been due to slow conversion of dt in dd during the recovery. In Antarctic diatoms, conversion of all dt into dd after high light exposure may take up to one hour causing slow relaxation of *NPQ* that is not due to damage to PS II (Kropuenske et al., 2009). Concurrently, significant amounts of dt were observed in the H treatment of the incubation experiment on station 250, approximately 30 min after the incubation ended. However, little ($<7\%$ of dd) or no dt was observed in any other samples, showing slow conversion of dd into dt did not affect relaxation in the other experiments. Alternatively, the slow relaxation in lincomycin treated samples may have been due to state transitions or *qT*. *qT* was demonstrated in some phytoplankton lineages (cyanobacteria, red algae, green algae), but not in diatoms. In higher plants *qT* was mainly relevant in low light

environments (Ruban and Johnson, 2009). However, in green algae $qT$ seemed a significant mechanism for acclimation to fluctuations in irradiance levels (Van Leeuwe et al., 2005).

The short-term SIE conditions resulted in the reduction of PS II efficiency for up to two hours. This photodamage incurred under relatively mild irradiance conditions confirms earlier studies showing that phytoplankton cells that are growing in a deeply mixed water column of the Southern Ocean are not adequately protected from photodamage by the irradiance conditions they encounter when mixed up to the surface and that D1 repair is crucial in maintaining photosynthetic performance under fluctuating irradiance conditions (Helbling et al., 1992; Alderkamp et al., 2010).

The increased $(dd+dt)$:Chl $a$ ratios in S samples when compared to D samples did not lessen photodamage when phytoplankton cells were exposed to excessive irradiance levels in the SIE experiments. Only small differences were observed in the $F_v/F_m$ recovery after exposure to excessive irradiance in samples from these two depths, similar to what was observed in the Atlantic region of the ACC (Alderkamp et al., 2010). Thus, the photoacclimation processes, such as xanthophyll synthesis, that were observed on time scales of vertical mixing in the UML are insufficient to protect against exposure to excessive irradiance.

Similar to the results within the UML, phytoplankton acclimated for six hours at 50% of incident irradiance (H) did not diminish photoinhibitory effects of surface irradiance exposure when compared to cells that were incubated at low irradiance (L: 2% of surface irradiance). Differences in $(dd+dt)$:Chl $a$ ratios confirmed xanthophyll cycle pigment synthesis, but this did not affect the $F_v/F_m$ recovery after exposure to excessive irradiance. In fact, $F_v/F_m$ recovery was sometimes faster in L incubations despite a lower $(dd+dt)$:Chl $a$ ratio than the H incubations. This surprising result may be due to the accumulation of photodamage incurred during the H incubation. As phytoplankton cells are exposed to supraoptimal levels of irradiance for longer times, the number of damaged proteins increases steadily (Van de Poll et al., 2005, 2007). The rather short time between the incubation and the surface irradiance exposure experiment ( < 1 h) likely did not allow for repair of all photodamaged proteins, which is consistent with the low initial levels of $F_v/F_m$ of the H samples in the surface irradiance exposure experiment. Thus, the potential positive effects of photoacclimation during six hours of acclimation may have been offset by the accumulation of photodamage.

To simulate exposure of phytoplankton to the irradiance levels they encounter in the upper water column, UV-B was omitted from our surface irradiance exposure experiments. The extinction coefficient of UV-B is higher than that of PAR and UV-A (Fry, 2000; Tedetti and Sempéré, 2006). However, when phytoplankton cells are mixed up to the upper few meters of the water column they will be exposed to significant levels of UV-B. Most reports suggest that photodamage in phytoplankton cells increased slightly in the presence of the natural component of UV-B when compared to exposure to UV-A and PAR alone (Helbling et al., 1992; Villafañe et al., 2003; Bouchard et al., 2005b). Thus, the photodamage observed in the surface irradiance exposure experiments may have been underestimated when compared to exposure to the full irradiance spectrum phytoplankton cells may encounter.

### 4.4. Photoacclimation in deeply mixed water columns

In general, *in situ* $F_v/F_m$ values vary with community structure, as well as physiological changes in phytoplankton (Sosik and Olson, 2002; Suggett et al., 2009). The $F_v/F_m$ was reduced with decreasing latitude and with the increasing contribution of chromophytes and nanoflagellates that accompanied the decreasing contribution of diatoms to the phytoplankton biomass. Similarly, in the six-hour H incubation experiments, the decline of $F_v/F_m$ became stronger as the contribution of chromophytes and nanoflagellates increased and diatoms decreased. These observations confirm the taxon-specific differences in photoacclimation to fluctuating irradiance reported previously in laboratory experiments with Antarctic phytoplankton. Van Leeuwe et al. (2005) showed that down-regulation of $F_v/F_m$ during high light exposure was stronger in the flagellate *Pyramimonas* than in the diatom *Chaetocesos brevis* under a sinusoidal light cycle and in fluctuating irradiance that mimicked slow vertical mixing. Under rapid irradiance fluctuations, however, no differences in fluorescence quenching were reported between the two taxa (Van Leeuwe et al., 2005), similar to the parallel responses by different phytoplankton communities to short-term surface irradiance exposure experiments in our study.

Within a mixed water column, net phytoplankton population growth will be positive provided that the depth-integrated photosynthetic rate is greater than the depth-integrated community loss terms, including grazing, sinking, cell death, and metabolic costs such as respiration (Sverdrup, 1953; Smetacek and Passow, 1990; Siegel et al., 2002). The $E_{UML}$ levels in the Drake Passage were low, with a mean of 1.7 mol photons $m^{-2}$ $day^{-1}$ (Fig. 3C), resulting in low photosynthetic rates. There is a metabolic cost associated with constant pigment synthesis as well as other photoacclimation mechanisms that increase the overall metabolic costs for phytoplankton growing under fluctuating irradiance (Dimier et al., 2009a). In addition, repair of photodamage to photosystems is an energetically expensive process (Aro et al., 1993; Hazzard et al., 1997), which limits allocation of energy to growth. Moreover, photosynthetic efficiency in our experiments was diminished for considerable time after exposure to surface irradiance. This will decrease the photosynthetic rate when phytoplankton is mixed down to depths that no longer cause photodamage. Thus, the increased metabolic costs due to constant pigment synthesis and PS II repair, in addition to diminished photosynthetic rates due to photodamage to PS II, will weigh heavy on phytoplankton growing under low mean irradiance levels (Ibelings et al., 1994; Alderkamp et al., 2010).

The results presented in this study provide evidence for xanthophyll cycle pigment synthesis within the UML by phytoplankton growing under low $E_{UML}$ throughout the Drake Passage. Therefore, xanthophyll cycling seems to be a significant mechanism for oceanic phytoplankton to deal with rapid changes in irradiance in HNLC regions with strong wind-induced vertical mixing. Nonetheless, higher levels of xanthophyll cycle pigments in phytoplankton at the top of the UML or in deck incubations under high irradiance did not lessen the photodamage incurred when phytoplankton were exposed to excessive irradiance levels. Photodamage affected phytoplankton exposed to irradiance levels at or below those encountered in the top 30 m of the water column during the local midday. Thus, paradoxically, photoinhibition may limit phytoplankton growth in HNLC regions with very low $E_{UML}$. Understanding the mechanisms of limitations to phytoplankton photosynthesis and, thus, primary productivity, by environmental factors in the Southern Ocean is critical if we are to accurately predict the impact of changes in Fe supply or $z_{UML}$ on its extent, e.g. due to climate change (Boyd et al., 2008). This knowledge eventually can be incorporated into regional and global models, resulting in greatly improved descriptions of Southern Ocean ecology and biogeochemistry and more reliable model predictions.

## References

Alderkamp, A.-C., de Baar, H.J.W., Visser, R.J.W., Arrigo, K.R., 2010. Can photo-inhibition control phytoplankton abundance in deeply mixed water columns of the Southern Ocean? Limnology and Oceanography 55, 1248–1264.

Amos, A.F., 2001. A decade of oceanographic variability in summertime near Elephant Island, Antarctica. Journal of Geophysical Research—Oceans 106, 22401–22423.

Aro, E.M., Mccaffery, S., Anderson, J.M., 1993. Photoinhibition and D1 protein degradation in peas acclimated to different growth irradiances. Plant Physiology 103, 835–843.

Behrenfeld, M.J., Bale, A.J., Kolber, Z.S., Aiken, J., Falkowski, P.G., 1996. Confirmation of iron limitation of phytoplankton photosynthesis in the equatorial Pacific Ocean. Nature 383, 508–511.

Bidigare, R.R., Smith, R.C., Baker, K.S., Marra, J., 1987. Oceanic primary production estimates from measurements of spectral irradiance and pigment concentrations. Global Biogeochemical Cycles 1, 171–186.

Bouchard, J.N., Campbell, D.A., Roy, S., 2005a. Effects of UV-B radiation on the D1 protein repair cycle of natural phytoplankton communities from three latitudes (Canada, Brazil, and Argentina). Journal of Phycology 41, 273–286.

Bouchard, J.N., Roy, S., Ferreyra, G., Campbell, D.A., Curtosi, A., 2005b. Ultraviolet-B effects on photosystem II efficiency of natural phytoplankton communities from Antarctica. Polar Biology 28, 607–618.

Boyd, P.W., Watson, A.J., Law, C.S., Abraham, E.R., Trull, T., Murdoch, R., Bakker, D.C.E., Bowie, A.R., Buesseler, K.O., Chang, H., Charette, M., Croot, P., Downing, K., Frew, R., Gall, M., Hadfield, M., Hall, J., Harvey, M., Jameson, G., Laroche, J., Liddicoat, M., Ling, R., Maldonado, M.T., Mckay, R.M., Nodder, S., Pickmere, S., Pridmore, R., Rintoul, S., Safi, K., Sutton, P., Strzepek, R., Tanneberger, K., Turner, S., Waite, A., Zeldis, J., 2000. A mesoscale phytoplankton bloom in the polar Southern Ocean stimulated by iron fertilization. Nature 407, 695–702.

Boyd, P.W., Doney, S.C., Strzepek, R., Dusenberry, J., Lindsay, K., Fung, I., 2008. Climate-mediated changes to mixed-layer properties in the Southern Ocean: assessing the phytoplankton response. Biogeosciences 5, 847–864.

Brunet, C., Casotti, R., Vantrepotte, V., 2008. Phytoplankton diel and vertical variability in photobiological responses at a coastal station in the Mediterranean Sea. Journal of Plankton Research 30, 645–654.

Chisholm, S.W., Morel, F.M.M., 1991. What controls phytoplankton production in nutrient-rich areas of the open sea? Limnology and Oceanography 36, U1507–U1511.

Cisewski, B., Strass, V.H., Prandke, H., 2005. Upper-ocean vertical mixing in the Antarctic Polar Front Zone. Deep-Sea Research II 52, 1087–1108.

Croot, P.L., Frew, R.D., Sander, S., Hunter, K.A., Ellwood, M.J., Pickmere, S.E., Abraham, E.R., Law, C.S., Smith, M.J., Boyd, P.W., 2007. Physical mixing effects on iron biogeochemical cycling: Fe cycle experiment. Journal of Geophysical Research—Oceans 112, L19606.

Cullen, J.J., Lewis, M.R., 1988. The kinetics of algal photoadaptation in the context of vertical mixing. Journal of Plankton Research 10, 1039–1063.

De Baar, H.J.W., Boyd, P.W., Coale, K.H., Landry, M.R., Tsuda, A., Assmy, P., Bakker, D.C.E., Bozec, Y., Barber, R.T., Brzezinski, M.A., Buesseler, K.O., Boye, M., Croot, P.L., Gervais, F., Gorbunov, M.Y., Harrison, P.J., Hiscock, W.T., Laan, P., Lancelot, C., Law, C.S., Levasseur, M., Marchetti, A., Millero, F.J., Nishioka, J., Nojiri, Y., van Oijen, T., Riebesell, U., Rijkenberg, M.J.A., Saito, H., Takeda, S., Timmermans, K.R., Veldhuis, M.J.W., Waite, A.M., Wong, C.S., 2005. Synthesis of iron fertilization experiments: from the iron age in the age of enlightenment. Journal of Geophysical Research—Oceans 110, C09S16.

Demmig, B., Winter, K., Kruger, A., Czygan, F.C., 1987. Photoinhibition and zeaxanthin formation in intact leaves—a possible role of the xanthophyll cycle in the dissipation of excess light energy. Plant Physiology 84, 218–224.

Demmig-Adams, B., Adams, W.W., 2006. Photoprotection in an ecological context: the remarkable complexity of thermal energy dissipation. New Phytologist 172, 11–21.

Demmig-Adams, B., 1990. Carotenoids and photoprotection in plants—a role for the xanthophyll zeaxanthin. Biochimica et Biophysica Acta 1020, 1–24.

Demmig-Adams, B., Adams, W.A., Logan, B.A., Verhoeven, A.S., 1995. Xanthophyll cycle-dependent energy dissipation and flexible photosystem II efficiency in plants acclimated to light stress. Australian Journal of Plant Physiology 22, 249–260.

Denman, K.L., Gargett, A.E., 1983. Time and space scales of vertical mixing and advection of phytoplankton in the upper ocean. Limnology and Oceanography 28, 801–815.

Dimier, C., Brunet, C., Geider, R., Raven, J., 2009a. Growth and photoregulation dynamics of the picoeukaryote Pelagomonas calceolata in fluctuating light. Limnology and Oceanography 54, 823–836.

Dimier, C., Giovanni, S., Ferdinando, T., Brunet, C., 2009b. Comparative ecophysiology of the xanthophyll cycle in six marine phytoplankton species. Protist 160, 397–411.

Falkowski, P.G., 1983. Light-shade adaptation and vertical mixing of marine phytoplankton: a comparative field study. Journal of Marine Research 41, 215–237.

Falkowski, P.G., La Roche, J., 1991. Acclimation to spectral irradiance in algae. Journal of Phycology 27, 8–14.

Fry, E.S., 2000. Visible and near-ultraviolet absorption spectrum of liquid water: comment. Applied Optics 39, 2743–2744.

Geider, R.J., Laroche, J., Greene, R.M., Olaizola, M., 1993. Response of the photosynthetic apparatus of Phaeodactylum tricornutum (Bacillariophyceae) to nitrate, phosphate, or iron starvation. Journal of Phycology 29, 755–766.

Griffith, G.P., Vennell, R., Williams, M.J.M., 2010. An algal photoprotection index and vertical mixing in the Southern Ocean. Journal of Plankton Research 32, 515–527.

Hazzard, C., Lesser, M.P., Kinzie, R.A., 1997. Effects of ultraviolet radiation on photosynthesis in the subtropical marine diatom, Chaetoceros gracilis (Bacillariophyceae). Journal of Phycology 33, 960–968.

Helbling, E.W., Villafane, V., Ferrario, M., Holmhansen, O., 1992. Impact of natural ultraviolet-radiation on rates of photosynthesis and on specific marine-phytoplankton species. Marine Ecology Progress Series 80, 89–100.

Hiscock, M.R., Marra, J., Smith, W.O., Goericke, R., Measures, C., Vink, S., Olson, R.J., Sosik, H.M., Barber, R.T., 2003. Primary productivity and its regulation in the Pacific Sector of the Southern Ocean. Deep-Sea Research II 50, 533–558.

Hofmann, E.E., Klinck, J.M., Lascara, C.M., Smith, D.A., 1996. Water mass distribution and circulation west of the Antarctic Peninsula and including Bransfield Strait. In: Ross, R.M., Hofman, E.E., Queti, L.B. (Eds.), Foundations for Ecological Research West of the Antarctic Peninsula. American Geophysical Union, pp. 61–80.

Hsu, S.A., Meindl, E.A., Gilhousen, D.B., 1994. Determining the power-law wind-profile exponent under near-neutral stability conditions at sea. Journal of Applied Meteorology 33, 757–765.

Ibelings, B.W., Kroon, B.M.A., Mur, L.R., 1994. Acclimation of photosystem-II in a cyanobacterium and a eukaryotic green-alga to high and fluctuating photosynthetic photon flux densities, simulating light regimes induced by mixing in lakes. New Phytologist 128, 407–424.

Kahru, M., Mitchell, B.G., Gille, S.T., Hewes, C.D., Holm-Hansen, O., 2007. Eddies enhance biological production in the Weddell-Scotia confluence of the southern ocean. Geophysical Research Letters 34, L14603.

Kana, R., Lazar, D., Prasil, O., Naus, J., 2002. Experimental and theoretical studies on the excess capacity of Photosystem II. Photosynthesis Research 72, 271–284.

Krause, G.H., Weis, E., 1991. Chlorophyll fluorescence and photosynthesis—the basics. Annual Review of Plant Physiology and Plant Molecular Biology 42, 313–349.

Kropuenske, L.R., Mills, M.M., van Dijken, G.L., Bailey, S., Robinson, D.H., Welschmeyer, N.A., Arrigo, K.R., 2009. Photophysiology in two major Southern Ocean phytoplankton taxa: photoprotection in Phaeocystis antarctica and Fragilariopsis cylindrus. Limnology and Oceanography 54, 1176–1196.

Kropuenske, L.R., Mills, M.M., Van Dijken, G.L., ALderkamp, A.-C., Berg, G.M., Robinson, D.H., Welschmeyer, N.A., Arrigo, K.R., 2010. Strategies and rates of photoacclimation in two major Southern Ocean phytoplankton taxa: Phaeocystis antarctica (haptophyta) and Fragilariopsis cylindrus (Bacillariophyceae). Journal of Phycology 46, 1138–1151.

Lavaud, J., Rousseau, B., Etienne, A.L., 2004. General features of photoprotection by energy dissipation in planktonic diatoms (Bacillariophyceae). Journal of Phycology 40, 130–137.

Lavaud, J., Strzepek, R.F., Kroth, P.G., 2007. Photoprotection capacity differs among diatoms: possible consequences on the spatial distribution of diatoms related to fluctuations in the underwater light climate. Limnology and Oceanography 52, 1188–1194.

Li, W.K.W., Smith, J.C., Platt, T., 1984. Temperature response of photosynthetic capacity and carboxylase activity in Arctic marine-phytoplankton. Marine Ecology Progress Series 17, 237–243.

MacIntyre, H.L., Kana, T.M., Geider, R.J., 2000. The effect of water motion on short-term rates of photosynthesis by marine phytoplankton. Trends in Plant Science 5, 12–17.

Maxwell, K., Johnson, G.N., 2000. Chlorophyll fluorescence—a practical guide. Journal of Experimental Botany 51, 659–668.

Middag, R., De Baar, H.J.W., Laan, P., Huhn, O. Journal of Geophysical Research—Oceans, submitted.

Mitchell, B.G., Brody, E.A., Holm-Hansen, O., Mcclain, C., Bishop, J., 1991. Light limitation of phytoplankton biomass and macronutrient utilization in the southern-ocean. Limnology and Oceanography 36, 1662–1677.

Moline, M.A., 1998. Photoadaptive response during the development of a coastal Antarctic diatom bloom and relationship to water column stability. Limnology and Oceanography 43, 146–153.

Neale, P.J., Helbling, E.W., Zagarese, H.E., 2003. Modulation of UVR exposure and effects by vertical mixing and advection. In: Helbling, E.W., Zagares, H.E. (Eds.), UV Effects in Aquatic Organisms and Ecosystems. The Royal Society of Chemistry, pp. 109–129.

Olaizola, M., Laroche, J., Kolber, Z., Falkowski, P.G., 1994. Nonphotochemical fluorescence quenching and the diadinoxanthin cycle in a marine diatom. Photosynthesis Research 41, 357–370.

Olaizola, M., Yamamoto, H.Y., 1994. Short-term response of the diadinoxanthin cycle and fluorescence yield to high irradiance in Chaetoceros muelleri (Bacillariophyceae). Journal of Phycology 30, 606–612.

Pollard, R.T., 1973. Wind driven mixing and deepening of oceanic boundary-layer. Quarterly Journal of the Royal Meteorological Society 99, 772–773.

Pollard, R.T., Lucas, M.I., Read, J.F., 2002. Physical controls on biogeochemical zonation in the Southern Ocean. Deep-Sea Research II 49, 3289–3305.

Ras, J., Claustre, H., Uitz, J., 2008. Spatial variability of phytoplankton pigment distributions in the Subtropical South Pacific Ocean: comparison between in situ and predicted data. Biogeosciences 5, 353–369.

Ross, O.N., Moore, C.M., Suggett, D.J., MacIntyre, H.L., Geider, R.J., 2008. A model of photosynthesis and photo-protection based on reaction center damage and repair. Limnology and Oceanography 53, 1835–1852.

Ruban, A.V., Johnson, M.P., 2009. Dynamics of higher plant photosystem cross-section associated with state transitions. Photosynthesis Research 99, 173–183.

Sakshaug, E., Holm-Hansen, O., 1986. Photoadaptation in Antarctic phyto-plankton—variations in growth-rate, chemical-composition and P-curve versus I-curve. Journal of Plankton Research 8, 459–473.

Schoemann, V., Becquevort, S., Stefels, J., Rousseau, V., Lancelot, C., 2005. *Phaeo-cystis* blooms in the global ocean and their controlling mechanisms: a review. Journal of Sea Research 53, 43–66.

Shelly, K., Heraud, P., Beardall, J., 2003. Interactive effects of PAR and UV-B radiation on PSII electron transport in the marine alga *Dunaliella tertiolecta* (Chlorophyceae). Journal of Phycology 39, 509–512.

Siegel, D.A., Doney, S.C., Yoder, J.A., 2002. The North Atlantic spring phytoplankton bloom and Sverdrup's critical depth hypothesis. Science 296, 730–733.

Smetacek, V., Passow, U., 1990. Spring bloom initiation and Sverdrup critical-depth model. Limnology and Oceanography 35, 228–234.

Sosik, H.M., Olson, R.J., 2002. Phytoplankton and iron limitation of photosynthetic efficiency in the Southern Ocean during late summer. Deep-Sea Research I 49, 1195–1216.

Strass, V.H., Garabato, A.C.N., Pollard, R.T., Fischer, H.I., Hense, I., Allen, J.T., Read, J.F., Leach, H., Smetacek, V., 2002. Mesoscale frontal dynamics: shaping the environment of primary production in the Antarctic Circumpolar Current. Deep-Sea Research II 49, 3735–3769.

Strzepek, R.F., Harrison, P.J., 2004. Photosynthetic architecture differs in coastal and oceanic diatoms. Nature 431, 689–692.

Suggett, D.J., Moore, C.M., Hickman, A.E., Geider, R.J., 2009. Interpretation of fast repetition rate (FRR) fluorescence: signatures of phytoplankton community structure versus physiological state. Marine Ecology Progress Series 376, 1–19.

Sverdrup, H.U., 1953. On conditions for the vernal blooming of phytoplankton. Journal du Conseil International pour l'Exploration de la Mer 18, 287–295.

Tedetti, M., Sempéré, R., 2006. Penetration of ultraviolet radiation in the marine environment. S review. Photochemistry and Photobiology 82, 389–397.

Tilzer, M.M., Dubinsky, Z., 1987. Effects of temperature and day length on the mass balance of Antarctic phytoplankton. Polar Biology 7, 35–42.

Tilzer, M.M., Elbrachter, M., Gieskes, W.W.C., Beese, B., 1986. Light-temperature interactions in the control of photosynthesis in Antarctic phytoplankton. Polar Biology 5, 105–111.

Uitz, J., Claustre, H., Morel, A., Hooker, S.B., 2006. Vertical distribution of phytoplankton communities in open ocean: an assessment based on surface chlorophyll. Journal of Geophysical Research—Oceans 111, C08005.

Van de Poll, W.H., Lagunas, M., De Vries, T., Visser, R.J.W., Buma, A.G.J., 2011. Non-photochemical quenching of chlorophyll fluorescence and xanthophyll cycle responses after excess PAR and UVR in *Chaetoceros brevis, Phaeocystis antarctica* and coastal Antarctic phytoplankton. Marine Ecology Progress Series 426, 119–131.

Van de Poll, W.H., Alderkamp, A.-C., Janknegt, P.J., Roggeveld, J., Buma, A.G.J., 2006. Photoacclimation modulates excessive photosynthetically active and ultravio-let radiation effects in a temperate and an Antarctic marine diatom. Limnology and Oceanography 51, 1239–1248.

Van de Poll, W.H., Janknegt, P.J., van Leeuwe, M.A., Visser, R.J.W., Buma, A.G.J., 2009. Excessive irradiance and antioxidant responses of an Antarctic marine diatom exposed to iron limitation and to dynamic irradiance. Journal of Photochemistry and Photobiology B Biology 94, 32–37.

Van de Poll, W.H., Van Leeuwe, M.A., Roggeveld, J., Buma, A.G.J., 2005. Nutrient limitation and high irradiance acclimation reduce PAR and UV-induced viability loss in the Antarctic diatom *Chaetoceros brevis* (Bacillariophyceae). Journal of Phycology 41, 840–850.

Van de Poll, W.H., Visser, R.J.W., Buma, A.G.J., 2007. Acclimation to a dynamic irradiance regime changes excessive irradiance sensitivity of *Emiliania huxleyi* and *Thalassiosira weissflogii*. Limnology and Oceanography 52, 1430–1438.

Van Donk, E., 2001. Aquatic plants and aquatic ecosystems. Plant Ecology 154, 247–259.

Van Leeuwe, M.A., Stefels, J., 2007. Photosynthetic responses in *Phaeocystis antarctica* towards varying light and iron conditions. Biogeochemistry 83, 61–70.

Van Leeuwe, M.A., Van Sikkelerus, B., Gieskes, W.W.C., Stefels, J., 2005. Taxon-specific differences in photoacclimation to fluctuating irradiance in an Ant-arctic diatom and a green flagellate. Marine Ecology Progress Series 288, 9–19.

Van Leeuwe, M.A., Villerius, L.A., Roggeveld, J., Visser, R.J.W., Stefels, J., 2006. An optimized method for automated analysis of algal pigments by HPLC. Marine Chemistry 102, 267–275.

Venables, H., Moore, C.M., 2010. Phytoplankton and light limitation in the South-ern Ocean: learning from high-nutrient, high-chlorophyll areas. Journal of Geophysical Research—Oceans 115, C02015.

Villafañe, V.E., Sundbäck, K., Figueroa, F.L., Helbling, E.W., 2003. Photosynthesis in the aquatic environment as affected by UVR. In: Helbling, E.W., Zagarese, H.E. (Eds.), UV Effects in Aquatic Organisms and Ecosystems. The Royal Society of Chemistry, pp. 357–397.

Walters, R.G., Horton, P., 1991. Resolution of components on non-photochemical chlorophyll fluorescence quenching in barley leaves. Photosynthesis Research 27, 121–133.

Whitworth, T., Nowlin, W.D., Orsi, A.H., Locarnini, R.A., Smith, S.G., 1994. Weddell Sea shelf water in the Bransfield Strait and Weddell-Scotia Confluence. Deep-Sea Research Part I 41, 629–641.